Hindawi Publishing Corporation
Journal of Nanomaterials
Volume 2012, Article ID 428643, 7 pages
doi:10.1155/2012/428643

Research Article

Urea-Based Combustion Process for the Synthesis of Nanocrystalline Ni-La-Fe-O Catalysts

Bahaa Abu-Zied[1,2] and Abdullah M. Asiri[1]

[1] *Center of Excellence for Advanced Materials Research, King Abdulaziz University, P.O. Box 80203, Jeddah 21589, Saudi Arabia*
[2] *Chemistry Department, Faculty of Science, Assiut University, Assiut 71516, Egypt*

Correspondence should be addressed to Bahaa Abu-Zied, babuzied@yahoo.com

Received 18 August 2012; Accepted 4 October 2012

Academic Editor: Fathallah Karimzadeh

Nanocrystalline Ni-La-Fe-O catalysts having the general formula $NiLa_xFe_{2-x}O_4$ ($0.00 \leq x \leq 2.00$) were synthesized by the combustion route employing urea as a combustion fuel. The calcination process was affected at 500°C. The structural properties of the obtained catalysts were systematically investigated by X-ray powder diffraction (XRD), scanning electronic microscopy (SEM), energy-dispersive X-ray spectra (EDX), and nitrogen adsorption at −196°C. Crystalline $NiFe_2O_4$ and La_2NiO_4 phases were detected for the catalysts having $x = 0.00$ and 2.00, respectively, as a result of solid-solid interaction between mixtures precursors. The activity of the obtained catalysts was checked for hydrogen peroxide decomposition at 35–55°C. A synergic effect was observed for the catalysts having x-value of 1.00 and 1.50. Such effect was attributed to the increase in the number of the active constituents involved in the catalytic decomposition of H_2O_2.

1. Introduction

Nickel ferrite, $NiFe_2O_4$, is one of the most important ferromagnetic materials which is known to exhibit low conductivity and thus lower eddy current losses, high electrochemical, thermal and chemical stability, abundance in nature, and so forth [1, 2]. $NiFe_2O_4$ has an inverse spinel structure in which the tetrahedral (A) sites are occupied by Fe^{3+} ions and the octahedral (B) sites are occupied by Ni^{2+} and Fe^{3+} ions in the spinel formula AB_2O_4 [3]. It has been widely used for various applications such as ferrofluids, catalysts, microwave devices, magnetic materials, gas sensors, high-density information storage, and as adsorbent to treat wastewater [4–6].

Lanthanum-nickelate-(La_2NiO_4-) based materials have attracted much attention in the past few years, as highly efficient electrochemical systems, including solid oxide fuel cells and ceramic membranes for oxygen separation and partial oxidation of hydrocarbons [7]. The La_2NiO_4 structure consists of alternating $LaNiO_3$ perovskite layers and LaO rock-salt layers with excess oxygen atoms occupying the interstitial sites between the LaO layers [7]. La_2NiO_4 exists over a broad range of oxygen nonstoichiometry and its structural, electrical, and magnetic properties are very sensitive to the amount of oxygen present [8].

The conventional ceramic method which involves the solid state reaction between the metal oxides, requiring a working temperature above 1000°C for several days, was commonly used for the preparation of $NiFe_2O_4$ [9]. Employing such high operating temperature lead to the formation of inhomogeneity, poor stoichiometry, and higher crystallite size $NiFe_2O_4$ spinel [10]. In agreement, it was reported that high temperature, 1100–1400°C or higher, is required for the preparation of La_2NiO_4 from its precursors oxides employing the ceramic method [11, 12].

Soft chemical processes such as sol-gel, precipitation, and combustion methods represent other alternative methods for the preparation of powder materials. Among the wet chemical methods, combustion process is known to be simple and cost effective and small crystallite size of the resultants, latter of which may have an important influence on the properties of the materials prepared [8, 13]. Its basic principle is to distribute metal ions throughout the polymeric network and to inhibit their segregation and

precipitation. Moreover, it involves an exothermic, generally very fast and self-sustaining chemical reaction between the desired metal salts and a suitable organic or inorganic fuel, which is ignited at temperatures much lower than the actual phase formation temperature [13].

To our knowledge in the open literature there is one paper dealing with the preparation and characterization of nano-crystalline $NiFe_{2-x}La_xO_4$, where the x-value was only limited to 0.09, which were synthesized by using metal nitrate and egg-white extract in aqueous medium [14]. Therefore, the present contribution was focused on the preparation and characterization of a series of nanocrystalline Ni-La-Fe-O catalysts via combustion synthesis. Five mixtures having the general formula $NiLa_xFe_{2-x}O_4$ (x = 0.00, 0.50, 1.00, 1.50, and 2.00) were prepared using urea as a combustion fuel. The molar ratio of urea/nitrate was adjusted to be 1. Calcination was affected, for 1 h, in static air atmosphere at 500°C. The obtained solids were characterized for their structure and surface morphology by means of X-ray diffraction (XRD), scanning electron microscopy (SEM), energy-dispersive X-ray spectra (EDX), and nitrogen adsorption at −196°C techniques. The crystallite size was calculated using XRD data and Scherrer's formula. The activity of the obtained catalysts towards H_2O_2 decomposition was tested.

2. Experimental

2.1. Catalysts Preparation. The reagents used in the materials preparation, $Ni(NO_3)_2{\cdot}6H_2O$, $Fe(NO_3)_3{\cdot}9H_2O$, $La(NO_3)_3{\cdot}6H_2O$, and urea were analytical grade chemicals. Five mixtures having the general formula $NiLa_xFe_{2-x}O_4$ (x = 0.00, 0.50, 1.00, 1.50, and 2.00) were prepared using urea as a combustion fuel. The molar ratio of urea/nitrate was adjusted to be 1. Prior to the calcination, the appropriate amounts of the reactants, with little added distilled water, were first mixed in a small porcelain crucible, then heated in an oven at 90°C. Finally, after the solution was converted to a viscous gel it was calcined, for 1 h, in air at 500°C, and then quenched to room temperature. During the first few minutes of the calcination process ignition took place with a rapid evolution of large amounts of gases. Therefore, only small portions of the gels were calcined.

2.2. Catalysts Characterization. XRD patterns of the calcination products were recorded using the powder diffraction pattern technique with 2θ ranging between 4 and 80°, with the aid of a Philips model PW 2103/00 diffractometer. The Philips generator, operated at 35 kV and 20 mA, provided a source of CuKα radiation. The FTIR spectra of the calcination products were recorded using the KBr disk technique in the range 4000–400 cm^{-1} using a Thermo-Nicolet-6700 FTIR spectrophotometer. Surface areas were determined by BET analysis of the corresponding nitrogen adsorption isotherms (at −196°C). The morphology of the samples was analyzed by field-emission scanning electron microscope (FE-SEM) on a JEOL model JSM-7600F microscope. The compositions were examined by energy-dispersive X-ray spectroscopy (EDX) in the SEM.

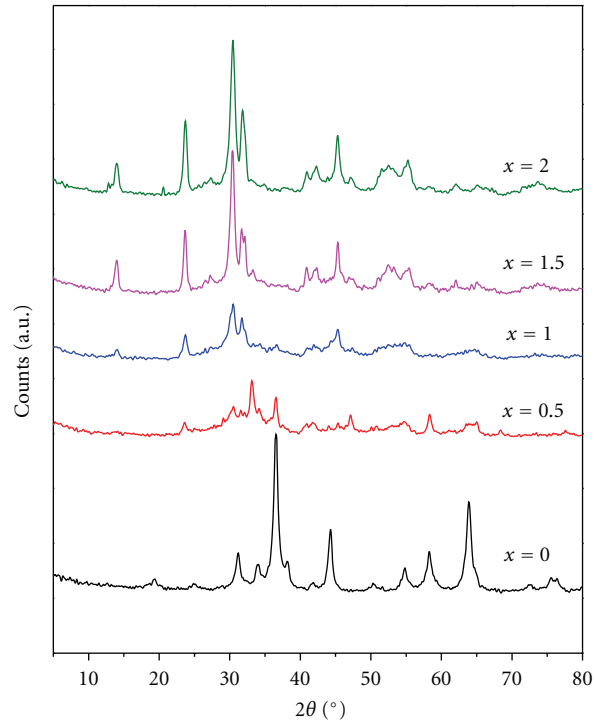

Figure 1: XRD patterns of the $NiLa_xFe_{2-x}O_4$ catalysts calcined at 500°C.

2.3. Activity Measurements. The measurements of the kinetics of catalytic decomposition of hydrogen peroxide have been carried out in a glass volumetric system. The measurements were conducted at 35–55°C temperature range. A constant catalyst weight 0.1 g was added to a thermostated reaction vessel containing 5 mL of hydrogen peroxide solution (30%, w/v). The analysis of the experimental data has been carried out on the assumption that the decomposition of H_2O_2 is a zero-order process. The pseudo-homogeneous zero-order rate constants, k_{hom}, have been calculated according to

$$V = V_0 + k_{hom}t, \tag{1}$$

where V is the volume of oxygen evolved at time t and V_0 is the volume of oxygen evolved to the moment at which the measurements started. The heterogeneous rate constant, k_{het}, is then calculated from k_{hom} as follows:

$$k_{het} = \frac{k_{hom}}{w \cdot S_{cat}}, \tag{2}$$

where w_{cat} is the weight of catalyst used and S_{cat} is the specific surface area of the catalyst.

3. Results and Discussion

3.1. Catalysts Characterization. X-ray diffraction patterns obtained for the calcination products of Ni-Fe-La-O mixtures formed in air at 500°C are shown in Figure 1. Inspection of this figure reveals, for x = 0.0, the existence

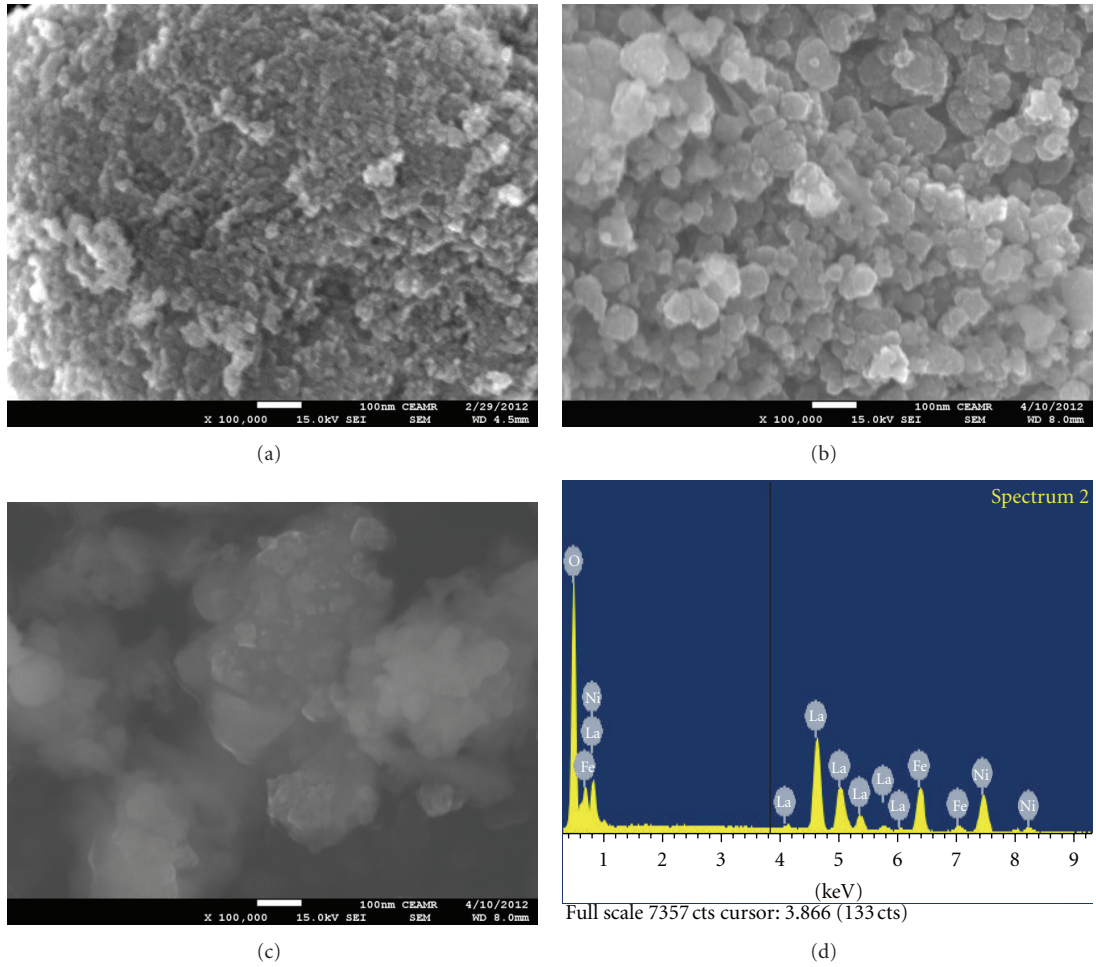

FIGURE 2: FE-SEM images of the $NiLa_xFe_{2-x}O_4$ catalysts, being calcined at 500°C, ($x = 0.00$ (a), $x = 01.00$ (b), and $x = 2.00$ (c)); EDX pattern of the SEM image of the catalyst with $x = 1.00$.

of $NiFe_2O_4$ as a major phase (JCPDS File no. 74-2081). Very week reflections attributable to Fe_2O_3 (JCPDS File no. 84-0311) were also detected. Increasing the x-value up to 2.00 is accompanied by a continuous decrease of the reflections due to $NiFe_2O_4$ together with the emergence of new ones assignable for the La_2NiO_4 phase (JCPDS File no. 80-1346). Moreover, trace amount of $La_2O_2CO_3$ (JCPDS File no. 23-0322) was also detected for the samples with high x-values. Two points could be raised in this respect: (i) employing urea as a combustion fuel favors the formation of the desired products ($NiFe_2O_4$ and La_2NiO_4) at temperatures as low as 500°C; (ii) the crystallinity of the obtained products decreases up on increasing x-value from 0.00 to 0.50, then it continuously increases with further x-value increase.

The crystallite sizes of the obtained catalysts were determined using the well-known Scherrer's formula on the basis of the full width of the diffraction line at half the maximum (FWHM) intensity measured in the most intense peak:

$$D = \frac{0.9\lambda}{\beta \cos\theta}, \quad (3)$$

where λ is the X-ray wavelength, θ isthe Bragg's angle and β is the full width of the diffraction line at half the maximum intensity. The obtained values are listed in Table 1.

TABLE 1: Crystallite sizes of the different $NiLa_xFe_{2-x}O_4$ catalysts calcined at 500°C.

Catalyst	$x = 0.00$	$x = 0.50$	$x = 1.00$	$x = 1.50$	$x = 2.00$
Crystallite size (nm)	9.75	6.26	13.62	18.39	14.29

Santos et al. [15] have reported an average crystallite size of 29 nm for nanosized $NiFe_2O_4$ powders being prepared by the combustion synthesis. Close value, 28 nm, was reported for sample synthesized via the thermal plasma method [16]. A value of 22 nm was reported for $NiFe_2O_4$ synthesized using sol-gel autocombustion [17] and ball milling [18] routes. Comparing the result of crystallite size for $NiFe_2O_4$ (around 10 nm) obtained in this work with the former reported values manifests the high efficiency of the combustion synthesis, employing urea as a fuel, in the preparation of nanosized

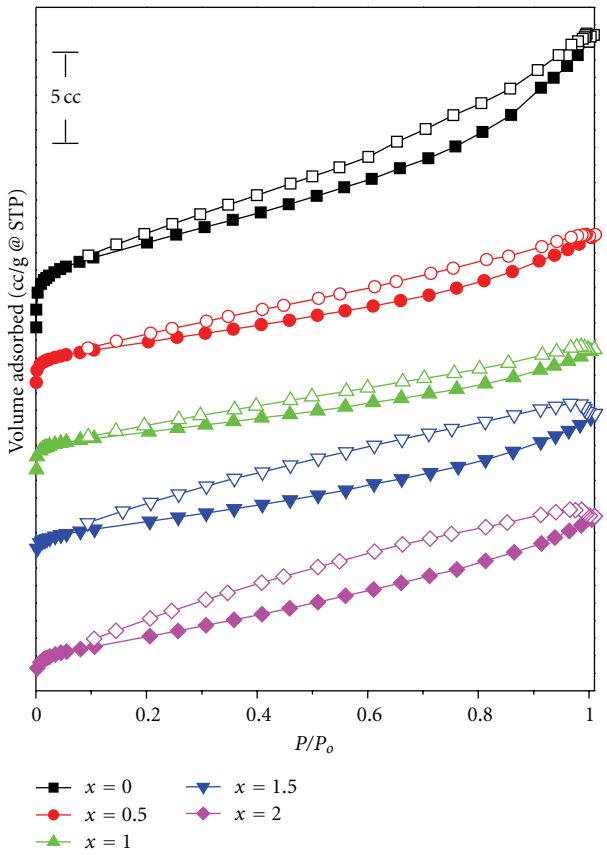

FIGURE 3: Nitrogen adsorption-desorption isotherms of the $NiLa_xFe_{2-x}O_4$ catalysts ($x = 0.00$, 0.50, 1.00, 1.50, and 2.00) catalysts.

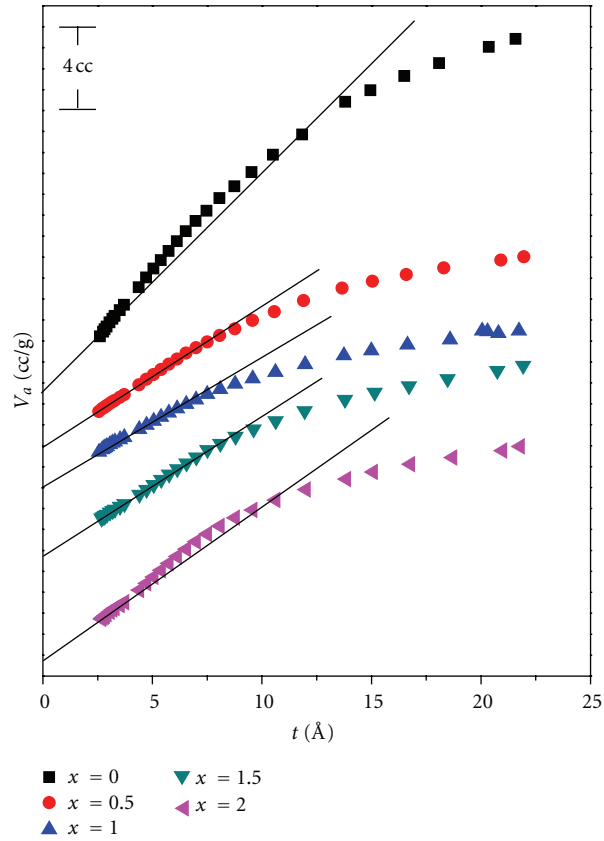

FIGURE 4: V_{a-t} plots for the $NiLa_xFe_{2-x}O_4$ catalysts ($x = 0.00$, 0.50, 1.00, 1.50, and 2.00) catalysts.

$NiFe_2O_4$ powders. In agreement, Vivekanandhan et al. [10] have reported a value of 14 nm for their $NiFe_2O_4$ being prepared via combustion process with metal nitrates as Ni and Fe ion sources and polyacrylic acid.

SEM micrographs of $NiLa_xFe_{2-x}O_4$ catalysts are depicted in Figure 2. The surface of the $NiFe_2O_4$ ($x = 0.00$), Figure 2(a), consists of a network of spherical particles seems to be practically uniform with average size 20–35 nm. The FE-SEM image of the $NiLaFeO_4$ catalyst, Figure 2(b), clarifies that this catalyst has bigger spheres like particles having a size in the range 25–100 nm. Moreover, irregular holes distributed among the various particles without a characteristic size or shape can be seen. Figure 2(c) indicates that the La_2NiO_4 catalyst consists of larger particles having irregular shape. SEM results suggest that the combustion technique, employing urea as fuel, is effective in terms of the preparation of nanocrystalline $NiLa_xFe_{2-x}O_4$ catalysts especially those having lower x-value with uniform structural properties. The EDX patterns of the synthesized $NiLa_xFe_{2-x}O_4$ catalysts were carried out to screen the composition of the metals. EDX analysis on several crystals revealed constancy of compositions. EDX analysis of the catalysts having $x = 0.00$ and 2.00 (not shown) indicates that the nanoparticles are composed of Ni and Fe for $NiFe_2O_4$ ($x = 0.00$) and Ni and La for La_2NiO_4 ($x = 2.00$). In addition, the atomic ratio of Fe/Ni and La/Ni is very close to 2 : 1. EDX analysis of $NiLaFeO_4$ catalyst, Figure 2(d), illustrates the coexistence of Ni, La, Fe, and O elements. Moreover, the Ni: Fe: La ratios were very close to 1 : 1 : 1.

Adsorption-desorption isotherms of nitrogen, measured at −196°C, over $NiLa_xFe_{2-x}O_4$ catalysts ($x = 0.00$, 0.50, 1.00, 1.50, and 2.00) are shown in Figure 3. On analyzing these isotherms it is possible to drive the specific area (S_{BET}), external surface area (S_t), the total pore volume (V_p), and the average pore diameter of each catalyst, as given in Table 2. The obtained isotherms are generally Type I according to Brunauer's classification [19] at low pressure values and a little of type II features at higher P/P_0 values. Moreover, the different catalysts exhibit a hysteresis loop nearly belongs to type H4 [19]. Furthermore, the closure point of the hysteresis loops for all the samples is approximately at $P/P_0 = 0.1$, which indicates either a strong affinity of adsorbate towards the surface or the existence of ultramicropores [20]. The specific surface areas were calculated by applying the BET equation, in its normal range of applicability, whereas S_t values were calculated using the V_{a-t} plots of de Bore [19].

The S_{BET} value of $NiFe_2O_4$, Table 2, is 19.73 m^2/g. It is evident that, increasing x-value leads to a continuous decrease of the S_{BET} value till $x = 1.50$, then it shows a slight increase on further x-value increase ($x = 2.00$). The obtained S_t values follow approximately similar trend. It is worth

Table 2: Textural data for the different $NiLa_xFe_{2-x}O_4$ catalysts.

Catalyst	S_{BET} (m^2/g)	External surface area (m^2/g)	Micropore surface area (m^2/g)	Total pore volume (cc/g)	Average pore radius (Å)
$x = 0.00$	19.73	17.57	2.16	0.02	17.27
$x = 0.50$	10.34	10.19	0.15	0.01	17.20
$x = 1.00$	9.68	8.28	1.40	0.01	15.38
$x = 1.50$	9.53	9.52	0.00	0.01	17.44
$x = 2.00$	11.28	11.28	0.00	0.01	17.16

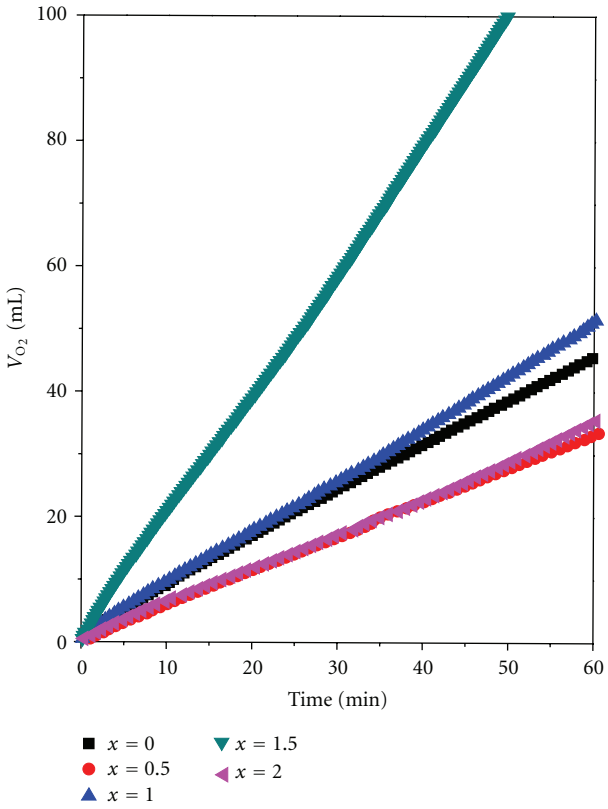

Figure 5: *V-t* plots for H_2O_2 decomposition obtained at 45°C over $NiLa_xFe_{2-x}O_4$ catalysts calcined at 500°C, where $x = 0.00$ (■), 0.50 (•),1.00 (▲), 1.50 (▼), and 2.00 (◄).

mentioning that, the obtained S_{BET} value of $NiFe_2O_4$ in this work is higher than that, 6.16 m^2/g, reported by Hou et al. [6]. Also, the obtained value for our La_2NiO_4, 14.29 m^2/g, is higher than that, 6.7 m^2/g, reported by Ramesh et al. [21].

The v_{a-t} plots characterizing the different $NiLa_xFe_{2-x}O_4$ catalysts are shown in Figure 4. It is evident that, both $NiFe_2O_4$ and La_2NiO_4 catalysts exhibit a mild positive deviation (upward deviation). This, in turn, indicates the mesoporous nature of both catalysts. At higher P/P_0 values the two curves show a negative deviation (downward deviation). Such behavior suggests the presence of microporous of both catalysts. The catalysts having $x = 0.50$, 1.00, and 1.50 exhibit microporous nature only as indicated by the downward deviations in the relevant v_{a-t} plots of these catalysts.

3.2. Activity Measurements. The kinetics of the catalytic decomposition of hydrogen peroxide was conducted at 35–55°C temperature range over the different $NiLa_xFe_{2-x}O_4$ catalysts calcined at 500°C. The treatment of the experimental data has been carried out on the assumption that the decomposition of H_2O_2 is a zero-order reaction. Thus, the volume of the evolved oxygen was recorded as a function of time. Figure 5 depicts the variation of the volume of oxygen evolved as a function of time at 45°C over all the catalysts. Straight lines were obtained and from the slope of these lines the relevant values of k_{hom} were obtained. In order to account for the induced changes in the specific surface area as a result of *x*-value change, the values of k_{hom} were converted to k_{het} for each catalyst at each reaction temperature and the obtained values were plotted as k_{het} versus *x*-value at different reaction temperatures as shown in Figure 6. From the inspection of this figure, it is obvious that increasing the temperature leads to a continuous increase in the obtained rate constant values for all the catalysts. Moreover, increasing the *x*-value is accompanied by an activity increase giving a maxima at $x = 1.5$. In other words, a synergic effect can be observed which is more pronounced for the catalyst with the composition $x = 1.50$.

Single transition metal oxides like NiO or Fe_2O_3 were reported to exhibit low activity towards hydrogen peroxide decomposition [22, 23]. On the other hand, higher activity patterns were reported for mixed transition metal oxides which are influenced by the ratio of the metal oxides in their mixtures as well as the presence of dopants. In this context, it was shown that the H_2O_2 decomposition activity of Cu : Fe mixed oxide varies in a nonmonotonic way with their composition [24]. The H_2O_2 decomposition activity, for the 350°C precalcined catalysts, was maximum for the mixtures rich in copper and iron species (3Cu : 1Fe and 1Cu : 3Fe). High H_2O_2 decomposition activity was reported over a series of $Ag/Fe_xAl_{2-x}O_3$ catalysts, being calcined at 300–700°C temperature range [13]. Irrespective of the calcination or the reaction temperatures, the highest activity was exhibited by catalyst having $x = 1.5$, that is, $Ag/Fe_{1.5}Al_{0.5}O_3$ catalyst. The activity of the Mn-oxide/Al_2O_3 catalysts, being calcined at 400–800°C, was greatly enhanced upon doping with Fe_2O_3 reaching a maximum value at 1.96%, then sharply decreases with further increase in iron content [22]. Concurrently, it was demonstrated that the addition of a very small amount of ZnO to the Co_3O_4/Al_2O_3 system led to an enhancement of its catalytic activity towards H_2O_2 decomposition [25].

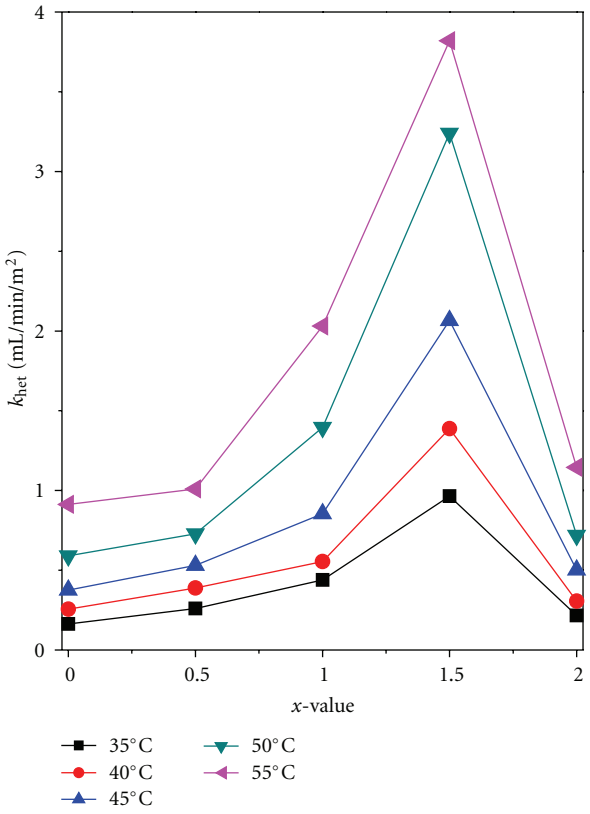

Figure 6: Variation of heterogeneous rate constant, k_{het}, values with x-values at reaction temperatures of 35 (■), 40 (•), 45 (▲), 50 (▼), and 55°C (◄) over $NiLa_xFe_{2-x}O_4$ catalysts calcined at 500°C.

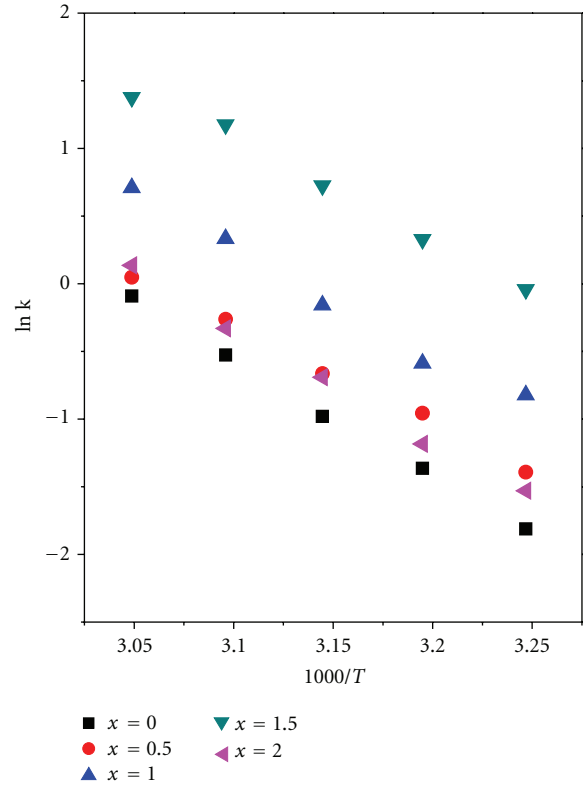

Figure 7: Arrhenius plots for H_2O_2 decomposition for the different $NiLa_xFe_{2-x}O_4$ catalysts calcined at 500°C.

The activity of mixed oxide catalysts during hydrogen peroxide decomposition is usually interpreted in terms of the concept of bivalent catalytic centres [14, 22–25]. In this way, for NiO/MgO doping with Fe_2O_3 it was suggested that, the doping effect did not modify the mechanism of H_2O_2 decomposition but rather formation of new active sites contributing in reaction. Such sites were believed to be ion pairs (Ni^{2+}-Fe^{3+}, Mg^{2+}-Fe^{3+}) [23]. For CuO-Fe_2O_3 catalysts, the higher catalytic activity of the two-component oxides was correlated, in addition to the one-component sites Cu^{2+}-Cu^{+} and Fe^{3+}-Fe^{2+} ions, to the newly formed mixed sites Cu^{2+}-Fe^{+} and/or Cu^{+}-Fe^{2+} ion pairs as a result of mutual charge interaction [24]. The H_2O_2 decomposition activity of mixed Fe_2O_3-MoO_3 catalyst, obtained by thermal treatment of the Fe-Mo mixtures at the same calcination temperature, was found to be greater than that of single oxides [26]. Such behavior was interpreted, also, in terms of the concept of bivalent catalytic centers. Thus, the higher catalytic activity of the two-component oxides was ascribed to the fact that beside the one-component sites Fe^{3+}-Fe^{2+} and Mo^{6+}-Mo^{5+}, there will also be the mixed sites Fe^{3+}-Mo^{5+} and/or Fe^{2+}-Mo^{6+} ion pairs as a result of mutual charge interactions [26].

Thus, in agreement with the above-mentioned literature data, the observed activity of $NiFe_2O_4$ and La_2NiO_4 catalysts, during H_2O_2 decomposition could be attributed to the mixed sites Ni^{2+}-Fe^{+3} and Ni^{2+}-La^{3+} ion pairs as a result of mutual charge interaction. Moreover, the synergic effect of mixing $NiFe_2O_4$ and La_2NiO_4, during H_2O_2 decomposition might be attributed to the increase in the concentration of active sites via creation of new ion pairs, probably Fe^{2+}-La^{3+} ion pair.

Figure 7 depicts the Arrhenius plots; ln k is related to the reciprocal absolute temperature, for H_2O_2 decomposition for the different $NiLa_xFe_{2-x}O_4$ catalysts. For the different catalysts, good linearity was obtained with correlation coefficients higher than 0.99. The obtained activation energy values were 71.8, 60.1, 66.8, 62.0, and 70.2 kJ/mol for the catalysts having $x = 0.00$, 0.50, 1.00, 1.50, and 2.00, respectively. The constancy of the obtained activation energy values suggests the similarity in nature of active centres over such catalysts series. Similar argument was suggested for H_2O_2 decomposition over other catalytic systems [24–26].

4. Conclusions

The results presented in this work showed that combustion synthesis, employing urea as combustion fuel, is a suitable and alternate method to prepare $NiLa_xFe_{2-x}O_4$ ($0.00 \leq x \leq 2.00$) catalysts at temperature as low as 500°C. $NiFe_2O_4$ and La_2NiO_4 represent the major phases for the catalysts having $x = 0.00$ and 2.00, respectively. The rest of the catalyst was found to be composed of a mixture of these two phases. However, impurities of iron oxide and lanthanum carbonate were detected. Kinetic studies of H_2O_2

decomposition reaction on this series of catalysts revealed a gradual activity increase accompanying the x-value increase passing a maxima at $x = 1.5$. In other words, a synergic effect was observed which is more pronounced for the catalysts having $x = 1.00$ and 1.50. Such effect could be anticipated to increase in the concentration of active sites throughout the formation of new ion pairs.

Acknowledgments

The authors are grateful to the Center of Research Excellence in Corrosion CoRE-C at King Fahd University for Petroleum and Mineral (KFUPM) for providing financial support for this work via Grant no. CR-7-2010. They also acknowledge the Center of Excellence for Advanced Materials Resaerch (CEAMR) at King Abdulaziz University for providing facilities.

References

[1] J. L. Gunjakar, A. M. More, K. V. Gurav, and C. D. Lokhande, "Chemical synthesis of spinel nickel ferrite ($NiFe_2O_4$) nanosheets," *Applied Surface Science*, vol. 254, no. 18, pp. 5844–5848, 2008.

[2] Z. Zhu, X. Li, Q. Zhao, H. Li, Y. Shen, and G. Chen, "Porous " brick-like" $NiFe_2O_4$ nanocrystals loaded with Ag species towards effective degradation of toluene," *Chemical Engineering Journal*, vol. 165, no. 1, pp. 64–70, 2010.

[3] N. M. Deraz, A. Alarifi, and S. A. Shaban, "Removal of sulfur from commercial kerosene using nanocrystalline $NiFe_2O_4$ based sorbents," *Journal of Saudi Chemical Society*, vol. 14, no. 4, pp. 357–362, 2010.

[4] V. Berbenni, C. Milanese, G. Bruni, and A. Marini, "The combined effect of mechanical and thermal energy on the solid-state formation of $NiFe_2O_4$ from the system $2NiCO_3 \cdot 3Ni(OH)_2 \cdot 4H_2O$-$FeC_2O_4 \cdot 2H_2O$," *Thermochimica Acta*, vol. 469, no. 1-2, pp. 86–90, 2008.

[5] J. D. A. Gomes, M. H. Sousa, F. A. Tourinho et al., "Synthesis of core-shell ferrite nanoparticles for ferrofluids: chemical and magnetic analysis," *Journal of Physical Chemistry C*, vol. 112, no. 16, pp. 6220–6227, 2008.

[6] X. Hou, J. Feng, X. Liu et al., "Synthesis of 3D porous ferromagnetic $NiFe_2O_4$ and using as novel adsorbent to treat wastewater," *Journal of Colloid and Interface Science*, vol. 362, no. 2, pp. 477–485, 2011.

[7] Y. H. Kim, S. M. Bae, C.-R. Park et al., "Indirect monitoring of mixed conduction in La2NiO4+δ-based systems using impedance spectroscopy," *Journal of Ceramic Processing Research*, vol. 12, no. 3, pp. 269–272, 2011.

[8] A. Demourgues, A. Wattiaux, J. C. Grenier et al., "Electrochemical preparation and structural characterization of $La_2NiO_{4+\delta}$ phases ($0 \leq \delta \leq 0.25$)," *Journal of Solid State Chemistry*, vol. 105, no. 2, pp. 458–468, 1993.

[9] F. Kenfack and H. Langbein, "Spinel ferrites of the quaternary system Cu-Ni-Fe-O: synthesis and characterization," *Journal of Materials Science*, vol. 41, no. 12, pp. 3683–3693, 2006.

[10] S. Vivekanandhan, M. Venkateswarlu, and N. Satyanarayana, "Effect of ethylene glycol on polyacrylic acid based combustion process for the synthesis of nano-crystalline nickel ferrite ($NiFe_2O_4$)," *Materials Letters*, vol. 58, no. 22-23, pp. 2717–2720, 2004.

[11] N. Yin, H. Wang, and C. Wang, "Effect of sintering temperature on morphology and arc erosion properties of La-Ni-O ceramic and its composites," *Journal of Rare Earths*, vol. 27, no. 3, pp. 506–509, 2009.

[12] M. Zinkevich, N. Solak, H. Nitsche, M. Ahrens, and F. Aldinger, "Stability and thermodynamic functions of lanthanum nickelates," *Journal of Alloys and Compounds*, vol. 438, no. 1-2, pp. 92–99, 2007.

[13] B. M. Abu-Zied, "Oxygen evolution over $Ag/Fe_xAl_{2-x}O_3$ ($0.0 \leq x \leq 2.0$) catalysts via N_2O and H_2O_2 decomposition," *Applied Catalysis A*, vol. 334, no. 1-2, pp. 234–242, 2008.

[14] Y. M. Al Angari, "Magnetic properties of La-substituted $NiFe_2O_4$ via egg-white precursor route," *Journal of Magnetism and Magnetic Materials*, vol. 323, no. 14, pp. 1835–1839, 2011.

[15] P. T. A. Santos, A. C. F. M. Costa, R. H. G. A. Kiminami, H. M. C. Andrade, H. L. Lira, and L. Gama, "Synthesis of a $NiFe_2O_4$ catalyst for the preferential oxidation of carbon monoxide (PROX)," *Journal of Alloys and Compounds*, vol. 483, no. 1-2, pp. 399–401, 2009.

[16] A. B. Nawale, N. S. Kanhe, K. R. Patil, S. V. Bhoraskar, V. L. Mathe, and A. K. Das, "Magnetic properties of thermal plasma synthesized nanocrystalline nickel ferrite ($NiFe_2O_4$)," *Journal of Alloys and Compounds*, vol. 509, no. 12, pp. 4404–4413, 2011.

[17] A. Ahlawat, V. G. Sathe, V. R. Reddy, and A. Gupta, "Mossbauer, Raman and X-ray diffraction studies of superparamagnetic $NiFe_2O_4$ nanoparticles prepared by solgel autocombustion method," *Journal of Magnetism and Magnetic Materials*, vol. 323, no. 15, pp. 2049–2054, 2011.

[18] S. Bid, P. Sahu, and S. K. Pradhan, "Microstructure characterization of mechanosynthesized nanocrystalline $NiFe_2O_4$ by Rietveld's analysis," *Physica E*, vol. 39, no. 2, pp. 175–184, 2007.

[19] G. Leofanti, M. Padovan, G. Tozzola, and B. Venturelli, "Surface area and pore texture of catalysts," *Catalysis Today*, vol. 41, no. 1–3, pp. 207–219, 1998.

[20] S. A. Soliman and B. M. Abu-Zied, "Thermal genesis, characterization, and electrical conductivity measurements of terbium oxide catalyst obtained from terbium acetate," *Thermochimica Acta*, vol. 491, no. 1-2, pp. 84–91, 2009.

[21] S. Ramesh, S. S. Manoharan, M. S. Hegde, and K. C. Patil, "Catalytic oxidation of ammonia to nitric-oxide over La_2MO_4 (M = Co, Ni, Cu) oxides," *Journal of Catalysis*, vol. 157, no. 2, pp. 749–751, 1995.

[22] W. M. Shaheen and K. S. Hong, "Thermal characterization and physicochemical properties of Fe_2O_3-Mn_2O_3/AL_2O_3 system," *Thermochimica Acta*, vol. 381, no. 2, pp. 153–164, 2002.

[23] W. M. Shaheen, A. A. Zahran, and G. A. El-Shobaky, "Surface and catalytic properties of NiO/MgO system doped with Fe_2O_3," *Colloids and Surfaces A*, vol. 231, no. 1–3, pp. 51–65, 2003.

[24] W. M. Shaheen and A. A. Ali, "Thermal solid-solid interaction and physicochemical properties of CuO-Fe_2O_3 system," *International Journal of Inorganic Materials*, vol. 3, no. 7, pp. 1073–1081, 2001.

[25] W. M. Shaheen and M. M. Selim, "Thermal characterization and catalytic properties of ZnO–Co_3O_4/Al_2O_3 system," *Afinidad*, vol. 58, no. 493, pp. 217–224, 2001.

[26] W. M. Shaheen, "Thermal behaviour of pure and binary $Fe(NO_3)_3 \cdot 9H_2O$ and $(NH_4)_6Mo_7O_{24} \cdot 4H_2O$ systems," *Materials Science and Engineering A*, vol. 445-446, pp. 113–121, 2007.